Perturbation-theory calculation of hyperfine structure in muonic helium

Sunil D. Lakdawala* and Peter J. Mohr
Gibbs Laboratory, Physics Department, Yale University, New Haven, Connecticut 06520
(Received 14 October 1983)

The lowest-order correction in the hyperfine splitting of muonic ^{4}He due to excitation of the effective $(\mu\text{-He})^+$ nucleus is precisely evaluated numerically. The result is $\Delta\nu_1^e=-45.670(8)$ MHz, in agreement with previous approximate analytic calculations. The mass-polarization correction to the hyperfine splitting is found to be $\Delta\nu_1^m=0.0785(2)$ MHz. The total perturbation-theory value for the hyperfine splitting is $\Delta\nu=4464.3(1.8)$ MHz, which is consistent with experiments at the Swiss Institute for Nuclear Research and at the Clinton P. Anderson Meson Physics Facility at Los Alamos.

I. INTRODUCTION

Studies of hyperfine structure in one-electron atoms have provided precise confirmations of quantum theory. In hydrogen, deuterium, and heavy atoms the hyperfine structure is quite accurately described by quantum electrodynamics with the assumption that the nucleus is pointlike. The composite structure of the nucleus is then a small correction based on parameters that account for the static distribution of nuclear charge and magnetization. The muonic helium atom, which consists of a helium nucleus, a negative muon, and an electron, is nearly hydrogenic. The helium nucleus and muon form a small inner atom with effective Bohr radius $a_\mu=(m_e/2m_\mu)a_e$, where a_e is the Bohr radius for the electron. This leads naturally to a theoretical description of the atom where in zeroth order the nucleus-muon system is regarded as pointlike, and structure corrections are treated as perturbations. In this approach excited states of the loosely bound nucleus-muon system make an important contribution to the hyperfine structure, in addition to the effect of the static distribution of charge and magnetization. From this point of view the muonic helium atom provides a system with known interactions in which we can study the effects of the composite structure and excited states of the effective nucleus on the hyperfine splitting.

The perturbation-theory approach has been applied within the context of the nonrelativistic Schrödinger equation that accounts for the dominant part of the hyperfine splitting. This approach can be generalized to give a quantum electrodynamic formulation for muonic helium that provides a consistent basis for the calculation of relativistic and radiative corrections.[1]

In this paper we examine the lowest-order excited-muon-state contribution to the muonic helium hyperfine structure. In previous work this quantity was calculated approximately analytically as a power series in m_e/m_μ by making plausible assumptions.[2] Here we confirm the validity of the approximations made in the analytic calculation by carrying out a complete numerical evaluation of the lowest-order excited-muon correction. The result improves the accuracy of the perturbation-theory evaluation of the muonic helium hyperfine structure and suggests that a more precise calculation based on this approach is feasible. The nonrelativistic mass-polarization correction to the hyperfine structure is evaluated with the same method. The calculation is described in detail in Secs. II–IV and in Sec. V the results are compared to other calculations and to experiment.

II. FORMULATION

To evaluate the hyperfine splitting we divide the Schrödinger Hamiltonian for the helium nucleus, muon, and electron into a zeroth-order part (units in which $\hbar=c=1$ are employed here)

$$H_0=-\frac{1}{2M_\mu}\nabla_\mu^2-\frac{1}{2M_e}\nabla_e^2-\frac{2\alpha}{x_\mu}-\frac{\alpha}{x_e}\ , \tag{1}$$

and perturbations

$$\delta V=\frac{\alpha}{x_{\mu e}}-\frac{\alpha}{x_e} \tag{2}$$

and

$$\delta M=-\frac{1}{m_N}\vec{\nabla}_\mu\cdot\vec{\nabla}_e\ . \tag{3}$$

In Eqs. (1)–(3), $\vec{x}_\mu$ and $\vec{x}_e$ are the coordinates of the muon and electron relative to the helium nucleus, and $M_\mu=m_\mu m_N/(m_\mu+m_N)$ and $M_e=m_e m_N/(m_e+m_N)$ are the reduced masses of the muon and electron relative to the nucleus. The nonrelativistic ground-state hyperfine splitting in muonic ^{4}He is given by[3]

$$\Delta\nu=\frac{2\pi\alpha}{3}\frac{g_\mu g_e}{m_\mu m_e}\langle\psi\,|\,\delta(\vec{x}_\mu-\vec{x}_e)\,|\,\psi\rangle\ , \tag{4}$$

where ψ is the ground-state eigenfunction of $H=H_0+\delta V+\delta M$.

In zeroth order in δV and δM, the eigenfunctions of H_0 are products of hydrogenic eigenfunctions for the muon and electron $\psi^{(0)}_{n,n'}=\psi_{\mu n}\psi_{en'}$, where $\psi_{\mu n}$ denotes the $(Z=2)$ muon state and $\psi_{en'}$ denotes the $(Z=1)$ electron state. The eigenvalues of H_0 are the sums of the hydrogenic eigenvalues $E^{(0)}_{n,n'}=E_{\mu n}+E_{en'}$. With the approximation $g_\mu=g_e=2$, the zeroth-order hyperfine splitting is

$$\Delta\nu_0=\frac{8\pi\alpha}{3}\frac{1}{m_\mu m_e}\langle\psi^{(0)}_{0,0}|\,\delta(\vec{x}_\mu-\vec{x}_e)\,|\psi^{(0)}_{0,0}\rangle\ . \tag{5}$$

It is convenient to divide the first-order correction in δV into two parts, corresponding to the intermediate-state muon in the ground state

$$\Delta\nu^g_1=\frac{16\pi\alpha}{3}\frac{1}{m_\mu m_e}\langle\psi^{(0)}_{0,0}|\,\delta(\vec{x}_\mu-\vec{x}_e)\times\sum_{n'\,(\neq 0)}\frac{|\psi^{(0)}_{0,n'}\rangle\langle\psi^{(0)}_{0,n'}|}{E^{(0)}_{0,0}-E^{(0)}_{0,n'}}\delta V\,|\psi^{(0)}_{0,0}\rangle\ , \tag{6}$$

or in excited states

$$\Delta\nu^e_1=\frac{16\pi\alpha}{3}\frac{1}{m_\mu m_e}\langle\psi^{(0)}_{0,0}|\,\delta(\vec{x}_\mu-\vec{x}_e)\times\sum_{\substack{n\,(\neq 0),\\ n'}}\frac{|\psi^{(0)}_{n,n'}\rangle\langle\psi^{(0)}_{n,n'}|}{E^{(0)}_{0,0}-E^{(0)}_{n,n'}}\delta V\,|\psi^{(0)}_{0,0}\rangle\ . \tag{7}$$

The first-order mass correction has a contribution only from intermediate states in which both the muon and electron are excited to P states

$$\Delta\nu^m_1=\frac{16\pi\alpha}{3}\frac{1}{m_\mu m_e}\langle\psi^{(0)}_{0,0}|\,\delta(\vec{x}_\mu-\vec{x}_e)\times\sum_{\substack{n\,(\neq 0),\\ n'\,(\neq 0)}}\frac{|\psi^{(0)}_{n,n'}\rangle\langle\psi^{(0)}_{n,n'}|}{E^{(0)}_{0,0}-E^{(0)}_{n,n'}}\delta M\,|\psi^{(0)}_{0,0}\rangle\ . \tag{8}$$

Thus the total first-order correction is

$$\Delta\nu_1=\Delta\nu^g_1+\Delta\nu^e_1+\Delta\nu^m_1\ . \tag{9}$$

An elementary evaluation yields the zeroth-order term

$$\Delta\nu_0=\Delta\nu_F\left[1+\frac{M_e}{2M_\mu}\right]^{-3}, \tag{10}$$

where

$$\Delta\nu_F=\frac{8}{3}\frac{\alpha(\alpha M_e)^3}{m_\mu m_e}\ . \tag{11}$$

The ground-state-muon correction is known accurately as[2]

$$\Delta\nu^g_1=\Delta\nu_F\left[\frac{11}{16}\frac{M_e}{M_\mu}+\left[\frac{M_e}{M_\mu}\right]^2\ln\left[\frac{M_\mu}{M_e}\right]-\frac{7}{64}\left[\frac{M_e}{M_\mu}\right]^2+O\left[\left[\frac{M_e}{M_\mu}\right]^3\ln\left[\frac{M_\mu}{M_e}\right]\right]\right]\ . \tag{12}$$

An approximate analytic calculation of $\Delta\nu^e_1$ has given the result[2]

$$\Delta\nu^e_1=\Delta\nu_F\left[-\frac{35}{16}\frac{M_e}{M_\mu}+\frac{2}{3}S_{1/2}\left[\frac{M_e}{M_\mu}\right]^{3/2}+O\left[\left[\frac{M_e}{M_\mu}\right]^2\ln\left[\frac{M_\mu}{M_e}\right]\right]\right], \tag{13}$$

where $S_{1/2}=2.8\pm0.2$. Amusia *et al.* have independently calculated a similar expansion for the hyperfine splitting.[4] Their results are consistent with Eqs. (10)–(13). An accurate numerical evaluation of $\Delta\nu^e_1$ and $\Delta\nu^m_1$ is described in the following sections.

III. EVALUATION OF $\Delta\nu^e_1$

In coordinate space, we have

$$\Delta\nu^e_1=\frac{16\pi}{3}\frac{\alpha^2}{m_\mu m_e}\int d\vec{x}_3\int d\vec{x}_2\int d\vec{x}_1\psi^\dagger_{\mu0}(\vec{x}_3)\psi^\dagger_{e0}(\vec{x}_3)\times\sum_{\substack{n\,(\neq 0),\\ n'}}\frac{\psi_{\mu n}(\vec{x}_3)\psi_{en'}(\vec{x}_3)\psi^\dagger_{\mu n}(\vec{x}_2)\psi^\dagger_{en'}(\vec{x}_1)}{E_{\mu0}+E_{e0}-E_{\mu n}-E_{en'}}\times\left[\frac{1}{x_{21}}-\frac{1}{x_1}\right]\psi_{\mu0}(\vec{x}_2)\psi_{e0}(\vec{x}_1)\ . \tag{14}$$

To facilitate the evaluation of (14), the summation over two-particle intermediate states is factorized into single-particle Coulomb Green's functions by means of the identity[5]

$$\sum_{\substack{n\,(\neq 0),\\ n'}}\frac{\psi_{\mu n}(\vec{x}_3)\psi_{en'}(\vec{x}_3)\psi^\dagger_{\mu n}(\vec{x}_2)\psi^\dagger_{en'}(\vec{x}_1)}{E_{\mu0}+E_{e0}-E_{\mu n}-E_{en'}}=\frac{1}{2\pi i}\int_{a-i\infty}^{a+i\infty}dz\sum_{n,n'}\frac{\psi_{\mu n}(\vec{x}_3)\psi^\dagger_{\mu n}(\vec{x}_2)}{z-(E_{\mu n}-E_{\mu0})}\frac{\psi_{en'}(\vec{x}_3)\psi^\dagger_{en'}(\vec{x}_1)}{z+(E_{en'}-E_{e0})}$$

$$=-\frac{1}{2\pi i}\int_{a-i\infty}^{a+i\infty}dzG_\mu(\vec{x}_3,\vec{x}_2,E_{\mu0}+z)G_e(\vec{x}_3,\vec{x}_1,E_{e0}-z)\ . \tag{15}$$

Figure 1 shows the singularities of the integrand in Eq. (15). The constant a is chosen such that the contour of integration passes between the two poles corresponding to the lowest two values of $E_{\mu n}-E_{\mu0}$:

$$0<a<\tfrac{3}{2}\alpha^2M_\mu\ . \tag{16}$$

For this choice of contour, terms in the integrand with $n=0$ and any n' vanish when integrated over z, since there are no singularities to the right of the contour in this case. Hence the summation in the integrand can be extended to all n and n'. The Green's functions in (15) are given by

$$G(\vec{x}_2,\vec{x}_1,z)=\sum_n\frac{\psi_n(\vec{x}_2)\psi^\dagger_n(\vec{x}_1)}{E_n-z} \tag{17}$$

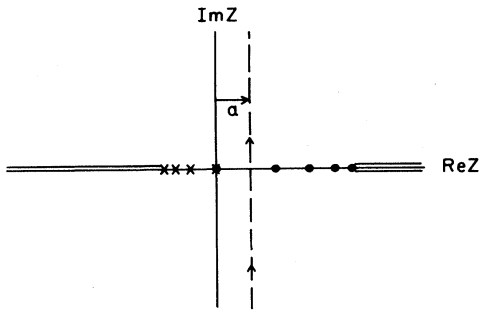

FIG. 1. Contour of integration and singularities of the integrand in the complex z plane for Eq. (15). The dashed line is the contour of integration, the crosses and double lines represent the discrete and continuous spectrum of the electron, respectively, and the solid circles and triple lines represent the discrete and continuous spectrum of the muon, respectively.

and they satisfy the equation

$$\left[-\frac{1}{2\mu}\nabla_2^2-\frac{Z\alpha}{x_2}-z\right]G(\vec{x}_2,\vec{x}_1,z)=\delta(\vec{x}_2-\vec{x}_1)\ , \tag{18}$$

with $\mu=M_\mu$ and $Z=2$ for the muon, and $\mu=M_e$ and $Z=1$ for the electron. The Coulomb Green's functions are expanded in eigenfunctions of angular momentum

$$G(\vec{x}_2,\vec{x}_1,z)=\sum_{l,m}G_l(x_2,x_1,z)Y_{lm}(\hat{x}_2)Y_{lm}^*(\hat{x}_1)\ , \tag{19}$$

with radial Green's functions G_l that satisfy the equation

$$\left[-\frac{1}{2\mu}\left[\frac{1}{x_2}\frac{d^2}{dx_2^2}x_2-\frac{l(l+1)}{x_2^2}\right]-\frac{Z\alpha}{x_2}-z\right]G_l(x_2,x_1,z)=-\frac{1}{x_2x_1}\delta(x_2-x_1)\ . \tag{20}$$

Construction of the radial Green's functions by well-known methods yields

$$G_l(x_2,x_1,z)=\frac{\mu}{cx_2x_1}\frac{\Gamma(1+l-\nu)}{\Gamma(2l+2)}M_{\nu,l+1/2}(2cx_<)\times W_{\nu,l+1/2}(2cx_>)\ , \tag{21}$$

where $M_{a,b}(x)$ and $W_{a,b}(x)$ are the Whittaker functions,[6] $c=(-2\mu z)^{1/2}$ with $\mathrm{Re}(c)>0$, $\nu=Z\alpha\mu/c$, and $x_<=\min(x_1,x_2)$, $x_>=\max(x_1,x_2)$. Substituting Eqs. (15) and (19) into (14) and integrating over coordinate angles, we obtain

$$\Delta\nu_1^e=\frac{2i}{3\pi}\frac{\alpha^2}{m_\mu m_e}\int_{a-i\infty}^{a+i\infty}dz\int_0^\infty dx_3x_3^2\int_0^\infty dx_2x_2^2\int_0^\infty dx_1x_1^2f_{\mu0}(x_3)f_{e0}(x_3)\times\sum_{l=0}^\infty G_{\mu l}(x_3,x_2,E_{\mu0}+z)G_{el}(x_3,x_1,E_{e0}-z)\times\left[\frac{x_<^l}{x_>^{l+1}}-\delta_{l0}\frac{1}{x_1}\right]f_{\mu0}(x_2)f_{e0}(x_1)\ , \tag{22}$$

where the functions $f_{\mu0}$ and f_{e0} are the zeroth-order ground-state radial wave functions for the muon and electron

$$f_0(x)=2(Z\alpha\mu)^{3/2}e^{-Z\alpha\mu x}\ . \tag{23}$$

To calculate numerically the radial Green's functions in (22) for a given range $l\le L$, the Whittaker functions in (21) are generated recursively in the index l. For numerical stability the functions M are calculated in the direction of decreasing l, and the functions W are calculated in the direction of increasing l. For the functions M we define

$$r_{\nu,l}(z)=\frac{M_{\nu,l+3/2}(z)}{M_{\nu,l+1/2}(z)}\ . \tag{24}$$

From the recurrence relations among the $M_{\nu,l+1/2}(z)$ one has[7]

$$\frac{1}{r_{\nu,l-1}(z)}=\frac{1}{z}-\frac{\nu}{2l(l+1)}+\frac{(l+1)^2-\nu^2}{4(l+1)^2(2l+1)(2l+3)}r_{\nu,l}(z)\ . \tag{25}$$

The recursion is initialized with the approximation

$$r_{\nu,L_m}(z)\approx z\ , \tag{26}$$

where

$$L_m=\max\{L,\ [\mathrm{Re}z/2]\}+[\mathrm{Re}z/20]+15\ . \tag{27}$$

The accuracy of successive $r_{\nu,l}(z)$ for decreasing l improves initially, such that the error in $r_{\nu,L}(z)$ for all relevant values of ν and z is less than 1 part in 10^5, as was determined by varying L_m. The $r_{\nu,l}(z)$ with $l<L$ then give the $M_{\nu,l+1/2}(z)$ up to a common constant factor. This constant is fixed by calculating $M_{\nu,11/2}(z)$ by numerically evaluating an integral representation for the function, as described in Appendix A. For the functions W, we define

$$u_{\nu,l}(z)=\frac{W_{\nu,l+3/2}(z)}{W_{\nu,l+1/2}(z)} \tag{28}$$

and from the recurrence relations among the $W_{\nu,l+1/2}(z)$,[7] one has

$$u_{\nu,l}(z)=\frac{2(l+1)(2l+1)}{l+1-\nu}\left[\frac{1}{z}-\frac{\nu}{2l(l+1)}+\frac{l+\nu}{2l(2l+1)}\frac{1}{u_{\nu,l-1}(z)}\right]. \quad (29)$$

The initial value $u_{\nu,0}(z)$ is obtained by numerically evaluating integral representations for $W_{\nu,1/2}(z)$ and $W_{\nu,3/2}(z)$, as described in Appendix B.

The summation over l in the integrand of (22) is carried out in two parts:

$$\sum_{l=0}^{\infty}F_l=\sum_{l=0}^{L}F_l+\sum_{l=L+1}^{\infty}F_l\ , \quad (30)$$

where

$$F_l=G_{\mu l}(x_3,x_2,E_{\mu 0}+z)G_{el}(x_3,x_1,E_{e0}-z)\times\left[\frac{x_<^l}{x_>^{l+1}}-\delta_{l0}\frac{1}{x_1}\right] \quad (31)$$

and

$$L=[2\max(|c_\mu|x_2,\ |c_\mu|x_3,\ |c_e|x_1,\ |c_e|x_3)]+10\ , \quad (32)$$

with $c_\mu=[-2(E_{\mu 0}+z)M_\mu]^{1/2}$, $\mathrm{Re}c_\mu>0$ and $c_e=[-2(E_{e0}-z)M_e]^{1/2}$, $\mathrm{Re}c_e>0$. The first sum on the right-hand side of (30) is evaluated exactly according to the preceding discussion. The second sum is approximated as follows. Each term in the sum is replaced by its asymptotic form A_l for large l (for $x_i<x_j<x_k$)

$$F_l\sim A_l=\frac{M_eM_\mu}{x_jx_k^2}\frac{r^l}{(l+1/2)^2}\ , \quad (33)$$

with $r=(x_i/x_k)^2$. The sum over l is approximated by writing

$$\sum_{l=L+1}^{\infty}\frac{r^l}{(l+1/2)^2}\approx\int_{L+1/2}^{\infty}dy\frac{r^y}{(y+1/2)^2}=\frac{1}{r^{1/2}}\frac{1}{L+1}E_2((L+1)\ln r^{-1}) \quad (34)$$

and the exponential integral function E_2 is numerically evaluated by known methods.[8] The accuracy of this method of calculating the sum was checked by comparing the results to the results obtained with the cutoff L replaced by $2L-10$ or $L+100$ for a representative sample of the variables x_1,x_2,x_3,z. The method appears to be accurate to better than 1 part in 10^4 based on this comparison.

Numerical integration over x_1,x_2,x_3,z in Eq. (22) is carried out as follows. Integration over z is replaced by integration over t where

$$z=2\alpha^2M_\mu[\kappa+i(t^{-2}-1)] \quad (35)$$

and our choice of

$$\kappa=\frac{a}{2\alpha^2M_\mu}=0.306 \quad (36)$$

is consistent with the inequality in (16). We thus have

$$\Delta\nu_1^e=\int_0^1 dt\,h(t)\ , \quad (37)$$

where

$$h(t)=\int_0^\infty dx_3\int_0^\infty dx_2\int_0^\infty dx_1U(x_3,x_2,x_1,t) \quad (38)$$

and

$$U(x_3,x_2,x_1,t)=-\frac{256}{\pi}\alpha^2(\alpha M_\mu)^4\Delta\nu_F x_3^2x_2^2x_1^2t^{-3}e^{-2\alpha M_\mu x_3}e^{-\alpha M_e x_3}e^{-2\alpha M_\mu x_2}e^{-\alpha M_e x_1}\times\mathrm{Re}\sum_{l=0}^{\infty}G_{\mu l}(x_3,x_2,E_{\mu 0}+z)G_{el}(x_3,x_1,E_{e0}-z)\left[\frac{x_<^l}{x_>^{l+1}}-\delta_{l0}\frac{1}{x_1}\right]. \quad (39)$$

For large values of the coordinates or Imz, the radial Green's functions are given approximately by[9]

$$G_l(x_2,x_1,z)\sim\frac{\mu}{cx_2x_1}\left[\frac{x_>}{x_<}\right]^\nu e^{-c|x_2-x_1|}\ . \quad (40)$$

Hence, for large Imz, or small t, the integrand in (38) has sharp peaks at $x_1=x_3$ and $x_2=x_3$. In addition, the cutoff L in (32) grows as $t\to 0$, increasing computer time and storage requirements for evaluation of the sum over l. In view of these facts, the function $h(t)$ is evaluated with two different methods depending on whether $0<t<0.05$ or $0.05<t<1$.

For the region $0.05<t<1$, the integration over x_3,x_2,x_1 is divided into six regions according to the relative magnitude of the three coordinates: $x_3<x_2<x_1$, $x_3<x_1<x_2$, etc. Then, for example, in the region with $x_3<x_2<x_1$, new variables of integration $y=x_1$, $r_1=x_2/x_1$, and $r_2=x_3/x_2$ are introduced giving

$$\int_0^\infty dx_1\int_0^{x_1}dx_2\int_0^{x_2}dx_3U(x_3,x_2,x_1,t)=\int_0^\infty dy\,y^2\int_0^1 dr_1r_1\int_0^1 dr_2U(r_1r_2y,r_1y,y,t)\ . \quad (41)$$

For large y we expect the asymptotic form of U to be given approximately by

$$|U|\propto e^{-Ay}\ , \quad (42)$$

where

$$A=\alpha M_e+\alpha(2M_\mu+M_e)r_1r_2+2\alpha M_\mu r_1+\mathrm{Re}(c_\mu)r_1(1-r_2)+\mathrm{Re}(c_e)(1-r_1r_2)\ , \quad (43)$$

as suggested by (39) and (40). This asymptotic form was verified numerically. Integration over y is facilitated by additional changes of variables

$$\int_0^\infty dy\, g(y)=\frac{1}{A}\int_0^\infty dy\, g(y/A)$$
$$=\frac{R}{A}\int_0^1 dy\, g(Ry/A)$$
$$+\frac{1}{A}\int_0^\infty dy\, g((R+y)/A)\ , \tag{44}$$

where $R=5$ and

$$g(y)=y^2U(r_1r_2y,r_1y,y,t)\ . \tag{45}$$

The first integral on the right-hand side of (44) is evaluated by 8-point Gauss-Legendre quadrature, and the second integral is evaluated by 8-point Gauss-Laguerre quadrature.[10] The integrals over r_1 and r_2 in (41) are each evaluated by Gauss-Legendre quadrature with 18 points for $0.05<t<0.1$ and 16 points for $0.1<t<1$. The coordinate integrations in the other five regions, $x_3>x_1>x_2$, etc., are evaluated in analogous fashion.

For $0<t<0.05$ the function $h(t)$ in Eq. (38) is replaced by a function $h_A(t)+\Delta h(t)$ that closely approximates $h(t)$. The function $h_A(t)$ is constructed so that

$$\lim_{t\to 0}\frac{h_A(t)}{h(t)}=1\ , \tag{46}$$

with two simplifying approximations in $h(t)$. First, the Green's functions for the electron and muon in Eq. (15) are replaced by the corresponding free Green's functions

$$G(\vec{x}_2,\vec{x}_1,z)\to G^{(0)}(\vec{x}_2,\vec{x}_1,z)=\frac{\mu}{2\pi}\frac{e^{-cx_{21}}}{x_{21}}\ , \tag{47}$$

with c as defined below Eq. (21). The fact that this replacement gives the leading behavior at small t (large $|z|$) is suggested by counting powers of z in the expansion

$$\frac{1}{H-z}=\frac{1}{H_0-z}-\frac{1}{H_0-z}V\frac{1}{H_0-z}+\cdots\ , \tag{48}$$

where $H=H_0+V$, H_0 is the free-particle Hamiltonian, and V is the Coulomb potential. Written in terms of the full Green's function $G(z)$ and the free Green's function $G^{(0)}(z)$, the expansion is

$$G(z)=G^{(0)}(z)-G^{(0)}(z)VG^{(0)}(z)+\cdots\ . \tag{49}$$

The second approximation is based on the fact that for large Imz, the quantity c in Eq. (47) has a large real part and so the free Green's functions are strongly peaked when the two coordinate arguments are equal. Thus, for large Imz, the leading contribution to the integral in (14) comes from the region $\vec{x}_1\approx\vec{x}_2\approx\vec{x}_3$, and we expect the replacement

$$\psi_{\mu 0}(\vec{x}_2)\psi_{e0}(\vec{x}_1)\to\psi_{\mu 0}(\vec{x}_3)\psi_{e0}(\vec{x}_3)$$

to be valid for the leading term. The validity of these approximations is more fully justified in Ref. 1. Combining Eqs. (14) and (15) and making these replacements we have

$$h_A(t)=-\frac{16\alpha^4M_eM_\mu^2}{3\pi^2m_em_\mu}t^{-3}\int d\vec{x}_3\int d\vec{x}_2\int d\vec{x}_1\,|\psi_{\mu 0}(\vec{x}_3)|^2|\psi_{e0}(\vec{x}_3)|^2\mathrm{Re}\left[\frac{e^{-c_\mu x_{32}}}{x_{32}}\frac{e^{-c_e x_{31}}}{x_{31}}\right]\left[\frac{1}{x_{21}}-\frac{1}{x_1}\right]\ . \tag{50}$$

With the aid of the identity

$$\int d\vec{x}_1\frac{e^{-cx_{31}}}{x_{31}x_{21}}=\frac{4\pi}{c^2}\frac{1}{x_{32}}(1-e^{-cx_{32}})\ , \tag{51}$$

the coordinate integrations in (50) are eliminated, with the result that

$$h_A(t)=\frac{256}{\pi}\Delta\nu_F\frac{\alpha^6M_eM_\mu^5}{s^3t^3}\mathrm{Re}\left[-\frac{1}{c_ec_\mu(c_e+c_\mu)}+\frac{s(4s+c_e)}{c_ec_\mu^2(2s+c_e)^2}\right]\ , \tag{52}$$

where $s=2\alpha M_\mu+\alpha M_e$. Numerically, the function $h_A(t)$ is qualitatively similar to $h(t)$. The fractional difference between $h_A(t)$ and $h(t)$ approaches zero as $t\to 0$, with typical values of 20% at $t=0.5$ and 4% at $t=0.1$. The remainder $\Delta h(t)$ is evaluated by fitting a third-degree interpolation polynomial to the calculated values of $h(t)-h_A(t)$ at the points $t=0$, 0.05, 0.09, and 0.12. The end-point value is $\Delta h(0)=0$, since $h(0)=h_A(0)=-303.21$ MHz.

The integral over t in Eq. (37) is evaluated by Gauss-Legendre quadrature with the above methods of calculating $h(t)$. The results are shown in Table I where the results for $\Delta\nu_1^e$ are tabulated as a function of the number of integration points N employed in the integration over t.

The numerical uncertainty in $\Delta\nu_1^e$ is estimated by integrating the pointwise uncertainty in the values for $h(t)$. In the range $0.1<t<1.0$, the calculation of $h(t)$ is designed at each stage to give an uncertainty of less than 1 part in 10^4, which corresponds to an error of 0.005 MHz in $\Delta\nu_1^e$. This accuracy is confirmed by observing the stability of $h(t)$ while varying the number of terms in the summation over l, varying the number of integration points in the evaluation of the functions M or W, or varying the number of integration points in the coordinate integrations. For $0.5<t<1.0$, the errors in $h(t)$ are much less than 0.005 MHz. For $0.05<t<0.5$, an independent error estimate for $h(t)$ is made by comparing the exact values of $h_A(t)$ given by Eq. (52) to the values obtained by the method employed to calculate $h(t)$ numerically, with the appropriate changes to give $h_A(t)$. The changes are to replace ν by 0 in the radial Green's functions and to replace the arguments of the wave functions by x_3 in Eq.

TABLE I. Numerical results for $\Delta\nu_1^e$.

Number of integration points N	$\Delta\nu_1^e$ (MHz)
4	−43.1346
6	−45.3567
8	−45.7640
10	−45.7172
12	−45.6796
14	−45.6708
16	−45.6702

(39). This comparison gives the numerical error in the evaluation of $h_A(t)$, which is expected to be of the same order of magnitude as the numerical error in the evaluation of $h(t)$. In the range $0.1<t<0.5$, the error in the numerical evaluation of $h_A(t)$ is less than 0.005 MHz. For $0.05<t<0.1$, the error in $h_A(t)$ increases as t decreases, to a value of about 0.035 MHz at $t=0.05$. To estimate the uncertainty in $\Delta h(t)$ in the range $0<t<0.05$, third-degree polynomials are fitted to the upper and lower estimated limits of the calculated values of $h(t)-h_A(t)$ at $t=0.05$, 0.09, and 0.12, with $\Delta h(0)=0$. The integrated error estimate is 0.008 MHz, so the result of the calculation is $\Delta\nu_1^e=-45.670(8)$ MHz.

Two additional consistency checks on the calculation have been made. For the 12-point integration over t, the calculation was done by the above method with the contour of integration over z in (22) shifted so that $\kappa=0.174$ [see Eq. (35)]. The result for $\Delta\nu_1^e$ agrees with the previous result within 1 part in 10^4. Also, a numerical calculation of $\Delta\nu_1^e$ was done with the same approximations as are made in the analytic calculation of Ref. 2. This numerical result agrees well with the analytic result.

IV. EVALUATION OF $\Delta\nu_1^m$

The mass-polarization correction in coordinate space reads

$$\Delta\nu_1^m=-\frac{32\pi}{3}\frac{\alpha^3M_\mu M_e}{m_N m_\mu m_e}\int d\vec{x}_3\int d\vec{x}_2\int d\vec{x}_1\psi_{\mu0}^\dagger(\vec{x}_3)\psi_{e0}^\dagger(\vec{x}_3)\sum_{\substack{n\,(\neq0),\\ n'\,(\neq0)}}\frac{\psi_{\mu n}(\vec{x}_3)\psi_{en'}(\vec{x}_3)\psi_{\mu n}^\dagger(\vec{x}_2)\psi_{en'}^\dagger(\vec{x}_1)}{E_{\mu0}+E_{e0}-E_{\mu n}-E_{en'}}$$
$$\times\hat{x}_2\cdot\hat{x}_1\psi_{\mu0}(\vec{x}_2)\psi_{e0}(\vec{x}_1)\ , \tag{53}$$

where the substitution

$$\vec{\nabla}_2\cdot\vec{\nabla}_1\psi_{\mu0}(\vec{x}_2)\psi_{e0}(\vec{x}_1)=2\alpha^2M_\mu M_e\hat{x}_2\cdot\hat{x}_1\psi_{\mu0}(\vec{x}_2)\psi_{e0}(\vec{x}_1) \tag{54}$$

has been made.

Proceeding in analogy with the treatment in Sec. III, we obtain

$$\Delta\nu_1^m=\int_0^1 dt\,h'(t)\ , \tag{55}$$

where

$$h'(t)=\frac{512}{\pi}\alpha^2\frac{M_e}{m_N}(\alpha M_\mu)^5\Delta\nu_F\int_0^\infty dx_3\int_0^\infty dx_2\int_0^\infty dx_1x_3^2x_2^2x_1^2t^{-3}e^{-2\alpha M_\mu x_3}e^{-\alpha M_e x_3}e^{-2\alpha M_\mu x_2}e^{-\alpha M_e x_1}$$
$$\times\mathrm{Re}[G_{\mu1}(x_3,x_2,E_{\mu0}+z)G_{e1}(x_3,x_1,E_{e0}-z)]\ . \tag{56}$$

In (56), only radial Green's functions with $l=1$ contribute, considerably simplifying the calculation.

For $0.1<t<1.0$, the coordinate integration in (56) is evaluated with the appropriate 22-, 8-, and 8-point quadrature method for integration over the variables r_1, r_2, and y, respectively, as defined in Sec. III.

For the range $0<t<0.1$, a function $h_A'(t)$ that approximates $h'(t)$ is constructed by making the approximations described in Sec. III to construct $h_A(t)$:

$$h_A'(t)=\frac{32\alpha^5M_e^2M_\mu^3}{3\pi^2m_em_\mu m_N}t^{-3}\int d\vec{x}_3\int d\vec{x}_2\int d\vec{x}_1\,|\,\psi_{\mu0}(\vec{x}_3)\,|^2\,|\,\psi_{e0}(\vec{x}_3)\,|^2\mathrm{Re}\left[\frac{e^{-c_\mu x_{32}}}{x_{32}}\frac{e^{-c_e x_{31}}}{x_{31}}\right]\hat{x}_2\cdot\hat{x}_1\ , \tag{57}$$

which yields

$$h_A'(t)=\frac{512}{\pi}\Delta\nu_F\frac{\alpha^7M_e^2M_\mu^6}{m_Nt^3}\mathrm{Re}\left[\frac{1}{s^3c_e^2c_\mu^2}-\frac{4}{sc_e^2c_\mu^2(2s+c_e)^2}-\frac{4}{sc_e^2c_\mu^2(2s+c_\mu)^2}+\frac{16}{c_e^3c_\mu^3(2s+c_e+c_\mu)}\right.$$
$$\left.+\frac{32s}{c_e^4c_\mu^4}\ln\left[\frac{2s(2s+c_e+c_\mu)}{(2s+c_e)(2s+c_\mu)}\right]\right]\ , \tag{58}$$

TABLE II. Numerical results for $\Delta\nu_1^m$.

Number of integration points N	$\Delta\nu_1^m$ (MHz)
4	0.078 87
6	0.078 53
8	0.078 52

where $s=2\alpha M_\mu+\alpha M_e$. For $0<t<0.1$, $h'(t)$ is approximated by $h'_A(t)$.

The numerical uncertainty in the calculated values of $h'(t)$ is estimated with the methods described in Sec. III. The error in the value of $h'(t)$ at $t=0.1$ is thus estimated to be 0.000 01 MHz, and the errors in $h'(t)$ for $0.1<t<1$ should be smaller. The difference between $h'_A(t)$ and $h'(t)$ at $t=0.1$ is 0.002 MHz, and this difference decreases as t decreases. Hence, approximating $h'(t)$ by $h'_A(t)$ in the region $0<t<0.1$ introduces an error smaller than 0.0002 MHz.

The results of evaluating the integral in (55) by Gauss-Legendre quadrature are shown, as a function of the number of integration points, in Table II. The result is $\Delta\nu_1^m=0.0785(2)$ MHz. An estimate of the order of magnitude for $\Delta\nu_1^m$ can be carried out analytically, yielding $\Delta\nu_1^m\approx\Delta\nu_F(M_e/m_N)(M_e/M_\mu)^{1/2}=0.04$ MHz, which is consistent with the numerical result.

V. CONCLUSION

The results of this calculation are $\Delta\nu_1^e=-45.670(8)$ MHz and $\Delta\nu_1^m=0.0785(2)$ MHz. The calculated value of $\Delta\nu_1^e$ is in agreement with and more accurate than the approximate analytic result in Eq. (13). The results of nonrelativistic perturbation theory for the hyperfine splitting in muonic ^{4}He are summarized in Table III. These numbers are based on the constants $R_\infty=3.289\,842\times10^9$ MHz, $\alpha^{-1}=137.0360$, $m_\mu/m_e=206.7686$, and $m_N/m_e=7294$, which yield $\Delta\nu_F=4516.91$ MHz. The uncertainty from the uncalculated second order in perturbation theory $\Delta\nu_2$ is estimated to be of order $\Delta\nu_F(M_e/M_\mu)^2\ln(M_\mu/M_e)$.[1] The total nonrelativistic result for the hyperfine splitting is 4453.8(1.2) MHz. This can be compared to the result of Huang and Hughes, 4455.1(0.3) MHz, based on a variational calculation,[11] and to the result of Drachman, 4450 MHz, obtained by a Born-Oppenheimer approximation method[12] and by a variational calculation in which the contact interaction is replaced by an equivalent global operator.[13]

TABLE III. Perturbation theory results for the hyperfine frequency.

MHz
$\Delta\nu_0=4483.38$
$\Delta\nu_\parallel^e=16.02$
$\Delta\nu_1^e=-45.67$
$\Delta\nu_1^m=0.08$
$\Delta\nu_2=\pm1.2$
total 4453.8(1.2) MHz

The main correction to the nonrelativistic result is due to the lowest-order anomalous magnetic moment of the electron and muon that together shift the hyperfine frequency by $\Delta\nu_F(\alpha/\pi)=10.5$ MHz. Relativistic and higher-order radiative corrections, both of order $\Delta\nu_F\alpha^2$, are not included here. The corresponding uncertainty is estimated to be 0.6 MHz. The total hyperfine splitting in muonic ^{4}He, based on perturbation theory, is $\Delta\nu=4464.3(1.8)$ MHz. This value is consistent with our previous result, $\Delta\nu=4462.6(3.0)$ MHz,[2] the result of Huang and Hughes, $\Delta\nu=4465.0(3)$ MHz,[11] and the result of Amusia *et al.*, $\Delta\nu=4462.9$ MHz.[4]

The theoretical values are in agreement with the measurement of $\Delta\nu$ in a weak magnetic field made at the Swiss Institute for Nuclear Research (SIN) $\Delta\nu=4464.95(6)$ MHz,[14] and with the results of the measurement of $\Delta\nu$ in a strong magnetic field made at the Clinton P. Anderson Meson Physics Facility at Los Alamos (LAMPF) $\Delta\nu=4465.004(29)$ MHz.[15]

ACKNOWLEDGMENT

This research was supported by the National Science Foundation, Grant No. PHY-80-26549.

APPENDIX A

We employ the integral representation

$$M_{\nu,l+1/2}(w)=\frac{\Gamma(2l+2)}{\Gamma(1+l+\nu)\Gamma(1+l-\nu)}w^{l+1}e^{-w/2}I\ , \tag{A1}$$

where

$$I=\int_0^1 dt\,t^{l-\nu}(1-t)^{l+\nu}e^{tw}\ , \tag{A2}$$

to evaluate numerically the function $M_{\nu,l+1/2}(w)$ for the range of parameters relevant to this calculation. This range lies within the boundaries $0<\mathrm{Re}\nu<1.2$; $l=5$; $\mathrm{Re}w>0$. For $0<\mathrm{Re}w<8$, the integral in (A2) is evaluated by 12-point Gauss-Legendre quadrature. For $8<\mathrm{Re}w<18$, the substitution $t=u^{1/2}$ is made in (A2), and the integral over u is evaluated by 12-point Gauss-Legendre quadrature. For $\mathrm{Re}w>18$ and $\mathrm{Im}w\neq0$, we introduce a new variable of integration $v=w(1-t)$ in (A2):

$$I=(e^w/w)\int_0^w dv\,(v/w)^{l+\nu}(1-v/w)^{l-\nu}e^{-v} \tag{A3}$$

and write

$$I=(e^w/w)\int_0^\infty dv\,(v/w)^{l+\nu}(1-v/w)^{l-\nu}e^{-v}+\epsilon\ , \tag{A4}$$

where

$$\epsilon=-\frac{1}{w}\int_0^\infty dv\,(1+v/w)^{l+\nu}(-v/w)^{l-\nu}e^{-v}\ . \tag{A5}$$

The integral in (A4) is evaluated by 10-point Gauss-

Laguerre quadrature. The correction ϵ is smaller than the main integral roughly by a factor $\exp(-\mathrm{Re}w)$, and its contribution is neglected in the evaluation of $M_{\nu,l+1/2}(w)$ with an error less than 1 part in 10^6.

APPENDIX B

To evaluate the function $W_{\nu,l+1/2}(w)$, we employ the representation

$$W_{\nu,l+1/2}(w)=\frac{1}{\Gamma(1+l-\nu)}w^l e^{-w/2}J\ , \tag{B1}$$

where

$$J=\int_0^\infty ds\,(s/w)^{l-\nu}(1+s/w)^{l+\nu}e^{-s}\ . \tag{B2}$$

The relevant parameters are within the range $0<\mathrm{Re}\nu<1.2$; $l=0,1$; $\mathrm{Re}w>0$. For $0<\mathrm{Re}w<0.35$, we write

$$J=\frac{\Gamma(1+l-\nu)}{w^{l-\nu}}\left[1+\frac{(l+\nu)(1+l-\nu)}{w}\right]+\int_0^1 ds(s/w)^{l-\nu}[(1+s/w)^{l+\nu}-1-(l+\nu)s/w]e^{-s}$$
$$+\int_0^\infty ds\left[\frac{s+1}{w}\right]^{l-\nu}\left[\left[1+\frac{s+1}{w}\right]^{l+\nu}-1-(l+\nu)\frac{s+1}{w}\right]e^{-(s+1)}\ . \tag{B3}$$

The first integral on the right-hand side of (B3) is evaluated by 10-point Gauss-Legendre quadrature, and the second integral is evaluated by 10-point Gauss-Laguerre quadrature. For $\mathrm{Re}w>0.35$, an additional term is extracted:

$$J=\frac{\Gamma(1+l-\nu)}{w^{l-\nu}}\left[1+\frac{(l+\nu)(1+l-\nu)}{w}+\frac{(l+\nu)(l+\nu-1)(1+l-\nu)(2+l-\nu)}{2w^2}\right]$$
$$+\int_0^1 ds\left[\frac{s}{w}\right]^{l-\nu}\left[\left[1+\frac{s}{w}\right]^{l+\nu}-1-(l+\nu)\frac{s}{w}-\frac{(l+\nu)(l+\nu-1)}{2}\left[\frac{s}{w}\right]^2\right]e^{-s}$$
$$+\int_0^\infty ds\left[\frac{s+1}{w}\right]^{l-\nu}\left[\left[1+\frac{s+1}{w}\right]^{l+\nu}-1-(l+\nu)\frac{s+1}{w}-\frac{(l+\nu)(l+\nu-1)}{2}\left[\frac{s+1}{w}\right]^2\right]e^{-(s+1)}\ . \tag{B4}$$

The integrals are evaluated as in (B3). In the final calculations of $\Delta\nu_1^e$, the number of integration points in the evaluation of $W_{\nu,l+1/2}(w)$ was taken as 5 instead of 10 to reduce the computation time. It was found empirically that this reduction did not affect the result within the desired level of precision (1 part in 10^4).

*Present address: Physics Department, Johns Hopkins University, Baltimore, MD 21218.

[1]S. D. Lakdawala, Ph.D. thesis, Yale University, 1982 (unpublished).

[2]S. D. Lakdawala and P. J. Mohr, Phys. Rev. A 22, 1572 (1980).

[3]H. A. Bethe and E. E. Salpeter, *Quantum Mechanics of One- and Two-Electron Atoms* (Springer, Berlin, 1957).

[4]M. Ya. Amusia, M. Ju. Kuchiev, and V. L. Yakhontov, J. Phys. B 16, L71 (1983).

[5]A similar identity is employed by M. O'Carroll and J. Sucher, Phys. Rev. Lett. 21, 1143 (1968).

[6]E. T. Whittaker and G. N. Watson, *A Course of Modern Analysis*, 4th ed. (Cambridge University, Cambridge, England, 1927).

[7]H. Buchholz, *The Confluent Hypergeometric Function* (Springer, Berlin, 1969).

[8]M. Abramowitz and I. A. Stegun, *Handbook of Mathematical Functions* (Dover, New York, 1965).

[9]W. Magnus, F. Oberhettinger, and R. P. Soni, *Formulas and Theorems for the Special Functions of Mathematical Physics* (Springer, New York, 1966).

[10]A. H. Stroud and D. Secrest, *Gaussian Quadrature Formulas* (Prentice-Hall, Englewood Cliffs, 1966).

[11]K. N. Huang and V. W. Hughes, Phys. Rev. A 26, 2330 (1982).

[12]R. J. Drachman, Phys. Rev. A 22, 1755 (1980).

[13]R. J. Drachman, J. Phys. B 14, 2733 (1981).

[14]H. Orth, K. P. Arnold, P. O. Egan, M. Gladisch, W. Jacobs, J. Vetter, W. Wahl, M. Wigand, V. W. Hughes, and G. zu Putlitz, Phys. Rev. Lett. 45, 1483 (1980).

[15]C. K. Gardner, A. Badertscher, W. Beer, P. R. Bolton, P. O. Egan, M. Gladisch, M. Greene, V. W. Hughes, D. C. Lu, F. G. Mariam, P. A. Souder, H. Orth, J. Vetter, and G. zu Putlitz, Phys. Rev. Lett. 48, 1168 (1982).